GMR
The Original

WOUND HEALING ACTIVITY OF MULTIFUNCTIONAL STARCH/PVA ELECTROSPUN NANOSCAFFOLDS INCORPORATED WITH ULTRASONIC-ASSISTED BIOGENIC SYNTHESIS OF CuO NANOPARTICLES FROM BROWN MARINE MACROALGAE (*Dictyota* sp.) EXTRACT

Elsa Sharon Emarald Ruban[1], Hari Shankar GG[2], Anand KH[3], Nishandhini Marimuthu[4], Kamaraj Raju[5]*

[1]Saveetha Medical College & Hospital (SMCH), Saveetha Institute of Medical and Technical Sciences (SIMATS), Thandalam, Chennai, Tamil Nadu 602105, India. elsasharon2004@gmail.com
[2]Department of Dermatology, Saveetha Medical College and Hospital, Saveetha Institute of Medical And Technical Sciences (SIMATS), Thandalam, Chennai-602105, Tamil Nadu, India. Email: Drharishankargg@gmail.com. ORCID: https://orcid.org/0009-0001-7695-1684.
[3]Department of ENT, Saveetha Medical College and Hospital, Saveetha Institute of Medical And Technical Sciences (SIMATS), Thandalam, Chennai-602105, Tamil Nadu, India. Email: anandkh91@gmail.com. ORCID: https://orcid.org/0000-0001-8496-5675.
[4]Department of Bioinformatics, School of Life Sciences, Vels Institute of Science Technology and Advanced Studies, Pallavaram,Chennai-600117, Tamil Nadu, India. Email: enishay30@gmail.com; ORCID: https://orcid.org/0000-0002-8536-4473
[5]School of Applied Biosciences, Food & Agri-Tech, Rathinam Global Deemed to be University, Coimbatore, 641021, Tamil Nadu, India. Email: kamaraj.lordshiva@gmail.com
*Correspondence: kamaraj.lordshiva@gmail.com (K.R.)

ABSTRACT
This study explores the wound healing potential of multifunctional starch/polyvinyl alcohol (PVA) electrospun nanoscaffolds incorporated with ultrasonically synthesized copper oxide nanoparticles (CuO NPs) derived from Dictyota sp. algal extract. UV-Vis spectroscopy confirmed nanoparticle formation, showing a characteristic surface plasmon resonance (SPR) peak, while Fourier-transform infrared spectroscopy (FTIR) and X-ray diffraction (XRD) analyses verified the chemical and crystalline structure of CuO NPs and their successful integration into the nanoscaffold matrix. Scanning electron microscopy (SEM) imaging revealed uniform nanoparticle distribution within smooth, bead-free nanofibers, and Thermogravimetric analysis (TGA) demonstrated enhanced thermal stability due to CuO NP incorporation. Dynamic light scattering (DLS) indicated stable, well-dispersed nanoparticles with a zeta potential of −20.08 mV. The wound healing (scratch) assay on HaCaT keratinocytes demonstrated concentration-dependent efficacy, with starch/PVA/CuO-NP nanoscaffolds outperforming both algal extract and CuO NPs alone. At 100 µg/mL, nanoscaffolds achieved 98.07% wound closure, compared to 86.07% for CuO NPs and 72.07% for algal extract. These results highlight the synergistic effect of the composite nanoscaffold in accelerating cell migration, positioning it as a promising biomaterial for advanced wound care applications. The study underscores the potential of green-synthesized CuO NPs and biopolymer-based nanoscaffolds in regenerative medicine.

KEYWORDS: *Dictyota* sp., Green synthesis, CuO nanoparticles, Starch/PVA/CuO-NPs nanoscaffolds, Wound-healing activity.

1. INTRODUCTION

Wound healing is a complex and dynamic physiological process involving a series of overlapping phases, including hemostasis, inflammation, proliferation, and remodeling, all of which are essential for restoring the integrity of damaged skin or tissues [1]. While minor injuries often heal naturally, chronic wounds caused by factors such as diabetes, infections, and vascular insufficiencies demand advanced therapeutic strategies [2]. In recent years, the field of regenerative medicine has focused increasingly on bioengineered wound dressings that not only protect the injured area but also accelerate healing by promoting cellular proliferation and minimizing infection risk [3]. Among the wide array of materials explored for such applications, biopolymer-based electrospun nanofibrous scaffolds have emerged as a promising class of wound dressings due to their structural similarity to the extracellular matrix (ECM), high surface area-to-volume ratio, and capability for sustained release of therapeutic agents [4].

Starch and polyvinyl alcohol (PVA) are two biocompatible and biodegradable polymers that have gained significant attention in the fabrication of nanofibrous scaffolds [5]. Starch, a naturally occurring polysaccharide, is widely available, non-toxic, and possesses inherent hydrophilicity, making it suitable for biomedical applications [6]. However, its mechanical limitations necessitate blending with other synthetic polymers such as PVA, which offers improved tensile strength and processability [7]. Electrospinning, a widely adopted technique for creating nanofibrous scaffolds, enables the fabrication of continuous fibers with controlled morphology and porosity [8]. When combined, starch and PVA can form a stable nanofibrous matrix capable of serving as a

functional scaffold for wound healing [9]. Moreover, these scaffolds can be further enhanced by the incorporation of metal-based nanoparticles, which exhibit potent antimicrobial and pro-regenerative activities [10].
Copper oxide nanoparticles (CuO NPs) have gained significant attention in biomedical research due to their broad-spectrum antimicrobial activity, low cytotoxicity at therapeutic doses, and essential role in angiogenesis and tissue repair [11]. Unlike silver or zinc oxide nanoparticles, CuO offers a cost-effective alternative with multifunctional properties [12]. Importantly, copper ions play a pivotal role in enzymatic reactions involved in collagen synthesis and cellular migration, both of which are essential for wound healing [13]. Conventional chemical synthesis of CuO NPs often involves toxic reducing agents or stabilizers that can hinder their biomedical applicability [14]. To overcome this limitation, green synthesis approaches have been introduced, leveraging the reducing and stabilizing capabilities of plant or algal extracts rich in bioactive compounds such as flavonoids, terpenoids, and phenolics [15].
Marine macroalgae, particularly brown algae such as Dictyota sp., are rich sources of bioactive secondary metabolites that make them ideal candidates for eco-friendly nanoparticle synthesis [16]. Dictyota sp. contains compounds with well-documented antioxidant, antimicrobial, and anti-inflammatory properties [17]. These bioactive molecules serve as natural capping and reducing agents, enabling the formation of nanoparticles under mild conditions without the use of toxic chemicals [18]. Moreover, the utilization of marine algae not only supports sustainable and renewable resource exploitation but also aligns with the principles of green chemistry and environmental stewardship [19].
In this context, the current research investigates the wound healing potential of starch/PVA electrospun nanofibrous scaffolds incorporated with CuO NPs synthesized via an ultrasonic-assisted green synthesis route using Dictyota sp. Extract [20]. Ultrasonic-assisted extraction enhances the release of intracellular compounds from the algal biomass, improving the efficiency and yield of nanoparticle synthesis [21]. The prepared CuO NPs were characterized using various physicochemical techniques to confirm their size, morphology, crystalline nature, and surface charge [22]. Subsequently, these nanoparticles were blended with starch and PVA solutions and electrospun into nanofibrous mats under optimized parameters [23]. The nanoscaffolds were evaluated for their structural integrity, thermal stability, and homogeneity of nanoparticle distribution [24].
To assess the biological efficacy of the fabricated nanofibers, an in vitro wound healing assay (scratch test) using HaCaT keratinocyte cells was conducted [25]. The assay measured cell migration and wound closure across different concentrations of test samples, including the algal extract, CuO NPs, and the final starch/PVA/CuO nanofibrous scaffolds [26]. The experimental data revealed significant enhancement in wound closure, especially in the nanoscaffold-treated groups, suggesting a synergistic effect between the bioactive components of the algae and the therapeutic properties of copper oxide. Additionally, statistical analyses were performed to ensure the validity and reliability of the results, with all observations interpreted within a 95% confidence interval.
The novelty of this research lies in the integration of green-synthesized CuO NPs with a biopolymer-based nanofibrous scaffold for wound healing applications [27]. While previous studies have explored the antimicrobial properties of CuO NPs or the biocompatibility of starch-PVA scaffolds separately, few have combined these approaches into a single multifunctional platform [20]. Furthermore, the use of Dictyota sp.—an underutilized brown macroalga—as a reducing and stabilizing agent adds an element of innovation and sustainability to the overall methodology [28].

2. MATERIALS AND METHODS

2.1 Chemicals and reagents

Dictyota, a brown marine alga, was harvested from the coastal regions near Rameswaram, Tamil Nadu, India, and employed as a sustainable source for biosynthesizing CuO NPs. Copper(II) sulfate pentahydrate ($CuSO_4 \cdot 5H_2O$), of analytical purity, served as the copper source. PVA with an approximate molecular weight of 115,000 g/mol and starch were selected as biopolymeric scaffold matrices. Nanofiber synthesis was carried out using the HOLMARC HO-NFES-040 electrospinning setup. All reagents and solvents used were of analytical grade and procured from Merck and Sigma-Aldrich to ensure experimental precision. Characterization methods included UV–visible spectroscopy, Fourier-transform infrared (FTIR) spectroscopy, X-ray diffraction (XRD), scanning electron microscopy (SEM), dynamic light scattering (DLS), zeta potential analysis, and thermogravimetric analysis (TGA). Standard protocols were followed to assess the in vitro wound-healing efficiency.

2.2 Collection and preparation of marine algae

Live Dictyota sp. samples were hand-collected from the intertidal area of Rameswaram's coast. Post-collection, the algae were stored in chilled conditions to preserve their bioactive constituents. The collected Dictyota was taxonomically identified and authenticated by Dr V. Veeragurunathan, CSIR-CSMCRI-Marine Algal Research Station, Mandapam Camp 623519, Tamil Nadu, India. A voucher specimen was prepared and deposited at the Herbarium of the CSIR-CSMCRI-Marine Algal Research Station, under the accession number: SI–2025–RMM–020. This authentication ensures botanical accuracy and standardization of the study material. The seaweed biomass underwent extensive rinsing with tap water to eliminate sediment and epiphytes, followed by repeated washing with distilled water to remove salt residues and other impurities. Approximately 100 grams of the cleaned specimens were sliced into smaller pieces and allowed to air-dry under ambient conditions for 14 days. Once

thoroughly dried, the material was pulverized into a fine powder using a mechanical grinder and preserved in airtight containers for subsequent extraction and nanoparticle biosynthesis.

2.3 Ultrasonic extraction of bioactive compounds

A 2 g portion of the dried algal powder was dispersed in 50 mL of Milli-Q water in a 100 mL borosilicate glass beaker. This suspension was subjected to ultrasonic extraction using a LABQUEST ultrasonic bath system (Borosil; Serial No. 941032329018) set at 60°C for 45 minutes to enhance the release of intracellular metabolites through acoustic cavitation. The extract was filtered through sterile Whatman No. 1 filter paper to remove solid residues. The resultant filtrate was stored at 10°C for later experiments, and part of the extract was lyophilized to produce a dry powder suitable for long-term storage and nanoparticle formation [29, 30].

2.4 Eco-friendly synthesis of CuO NPs

CuO NPs were synthesized by mixing 50 mL of 0.1 M copper sulfate solution with 10 mL of Dictyota extract (10 mg/mL) in a volumetric ratio of 5:1. The reaction mixture was stirred at 650 rpm and heated to 60°C for 2 hours. A change in color from deep blue to bluish-green confirmed nanoparticle formation, attributed to the phytochemical constituents of the extract. The synthesized product was washed three times with double-distilled water to remove residual organics and was freeze-dried over 48 hours to obtain CuO nanopowder for subsequent applications [31].

2.5 Synthesis of starch/PVA/CuO nanofibrous scaffolds

A 15% (w/w) PVA solution was created by dissolving the polymer in Milli-Q water under continuous stirring at 50°C. Following complete dissolution, 100 mg each of starch and CuO NPs were incorporated, and the mixture was further stirred at 50°C for 2.5 hours to ensure uniform dispersion. The homogenous blend was loaded into a syringe fitted with a 0.84 mm stainless steel nozzle. Electrospinning was performed using the HOLMARC HO-NFES-040 setup, applying a voltage of 11.5 kV, maintaining a 12.3 cm distance between the needle tip and the collector, and feeding at a rate of 0.4 mL/h. Electrospinning was continued for 6–8 hours at ambient conditions to yield fibrous mats, which were then stored in a desiccator pending further analyses [32-34].

2.6 Physicochemical characterization

2.6.1 UV–vis spectroscopy

Absorbance spectra of the Dictyota extract, synthesized CuO NPs, and fabricated nanofiber mats were measured using a VIS SPEC V-730 spectrophotometer. Spectra were scanned between 200 and 800 nm using deionized water as the blank. Absorption peaks within the 270–300 nm range were observed, indicating the surface plasmon resonance (SPR) typical of CuO NPs and suggesting their successful incorporation into the nanocomposite matrix [35].

2.6.2 FTIR spectroscopy

FIRD spectra were collected using a PerkinElmer Spectrum Two FTIR spectrometer equipped with an ATR unit. The analysis was carried out in the spectral range of 4000–400 cm^{-1} with a resolution of 4 cm^{-1}, averaged over 64 scans. The detected peaks corresponded to functional groups such as hydroxyl, carbonyl, amide, and metal–oxygen bonds, validating the presence of bioactive components and nanoparticle integration [36].

2.6.3 XRD analysis

Crystalline structure was examined using a Bruker D8 Advance diffractometer with CuKα radiation (λ = 1.5406 Å), operated at 40 kV and 40 mA. Scans were performed over a 2θ range of 5° to 90° with a step increment of 0.029649°. Distinct peaks corresponding to monoclinic CuO confirmed nanoparticle formation, while peak broadening in composite scaffolds reflected polymer embedding [37].

2.6.4 SEM analysis

The surface morphology of nanofibers was analyzed via JEOL JSM-IT800 NANO SEM. Prior to imaging, samples were coated with a thin layer of gold. SEM images revealed a uniform fiber network with consistent diameters and even distribution of CuO NPs, indicative of a successful electrospinning process [38].

2.6.5 TGA

Thermal decomposition behavior was evaluated using a PerkinElmer TGA 8000 system. Around 5 mg of each sample was heated from room temperature up to 550°C at a rate of 15°C/min under nitrogen. Weight loss stages revealed water evaporation, polymer breakdown, and thermal reinforcement provided by CuO NPs [39].

2.6.6 Particle size and zeta potential

Size distribution and surface charge of the synthesized nanoparticles were measured using a Malvern Zetasizer Ultra. Zeta potential values exceeding ±30 mV suggested high colloidal stability, reducing aggregation and promoting potential biomedical use. All raw and processed data are available in the Mendeley Data repository (DOI: 10.17632/xtwhbc25hj.2) for reference and validation [22].

2.7 Wound healing (scratch) assay

A scratch assay was conducted to assess the cell migration ability of HaCaT keratinocytes following treatment with Dictyota extract, CuO NPs, and starch/PVA/CuO nanofiber scaffolds. Cells were seeded in 12-well plates at a density of 2×10^5 cells per well in DMEM containing 10% FBS and 1% penicillin-streptomycin, and incubated

at 37°C with 5% CO_2 until confluence. A sterile 200 µL pipette tip was used to create a linear scratch in each well. Following PBS washing, cells were exposed to test samples at concentrations of 6.25, 12.5, 25, 50, and 100 µg/mL in serum-free DMEM. Wells without treatment acted as controls. Wound closure progression was photographed at 0, 24, and 48 hours using an inverted phase-contrast microscope. ImageJ software was employed to quantify cell migration and calculate the percentage of wound closure to compare treatment efficacies [40].

2.8 Statistical analysis

All experimental observations were subjected to statistical analysis using SPSS v25.0 and GraphPad Prism v9.0 software. Results from three independent trials were expressed as mean ± standard deviation. Group differences were determined using one-way ANOVA with appropriate post-hoc tests such as Tukey's or Dunnett's, depending on the context. A p-value of less than 0.05 was considered statistically significant. Pearson correlation coefficients were calculated to assess inter-variable relationships. Data normality was evaluated using the Shapiro–Wilk test, and log transformations were applied to non-normally distributed datasets. Statistical evaluations were carried out at a 95% confidence level [41].

3. RESULTS

3.1. UV–visible spectroscopy

The UV–Visible spectroscopic profile (Fig. 1) was recorded using a JASCO V-730 spectrophotometer over the 200–800 nm spectral range to evaluate both the Dictyota algal extract and the CuO NPs synthesized from it. The algal extract demonstrated a broad absorption band centered at 337 nm (absorbance = 1.482), signifying the existence of bioactive compounds like polyphenols. These molecules are presumed to play key roles in reducing and stabilizing the nanoparticles. In contrast, the CuO NPs showed a distinct absorbance peak between 270 and 300 nm, corresponding to surface plasmon resonance (SPR), which is typical for nanoscale materials. Additionally, the CuO NPs displayed an intense absorbance (2.369 at 800 nm), which progressively declined at lower wavelengths, aligning with known optical behavior of metallic oxides. These shifts in absorbance confirm the successful synthesis of CuO NPs and highlight the critical involvement of Dictyota-derived phytochemicals in the nanoparticle formation and capping processes.

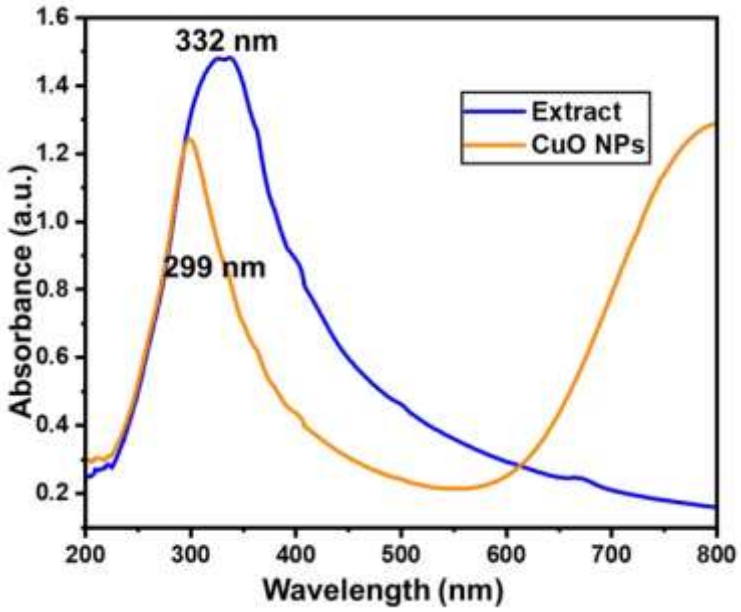

Fig. 1. UV–Visible spectral profiles of algal extract and CuO NPs**.**

3.2. FTIR analysis

FTIR spectroscopy (Fig. 2) was used to determine the chemical functionalities present in both CuO NPs and the CuO-embedded starch/PVA scaffolds. The CuO NPs displayed characteristic absorption peaks at 2033.36, 1640.64, and 594.02 cm^{-1}, which are assigned to Cu–O bond stretching, verifying the formation of copper oxide. Additional absorption features at 767.66 and 469.77 cm^{-1} further support the presence of copper–oxygen bonding. The scaffold matrix showed prominent bands at 3289.72 cm^{-1} for O–H stretching, 1426.07 cm^{-1} representing C–H bending, and 110.59 cm^{-1} linked to C–O–C stretching vibrations, corresponding to starch and PVA structures. Notably, absorption features in the 600–400 cm^{-1} region confirmed successful incorporation of CuO NPs into the polymeric system. Overall, these spectra suggest that embedding CuO NPs did not cause substantial alterations in the scaffold's chemical identity.

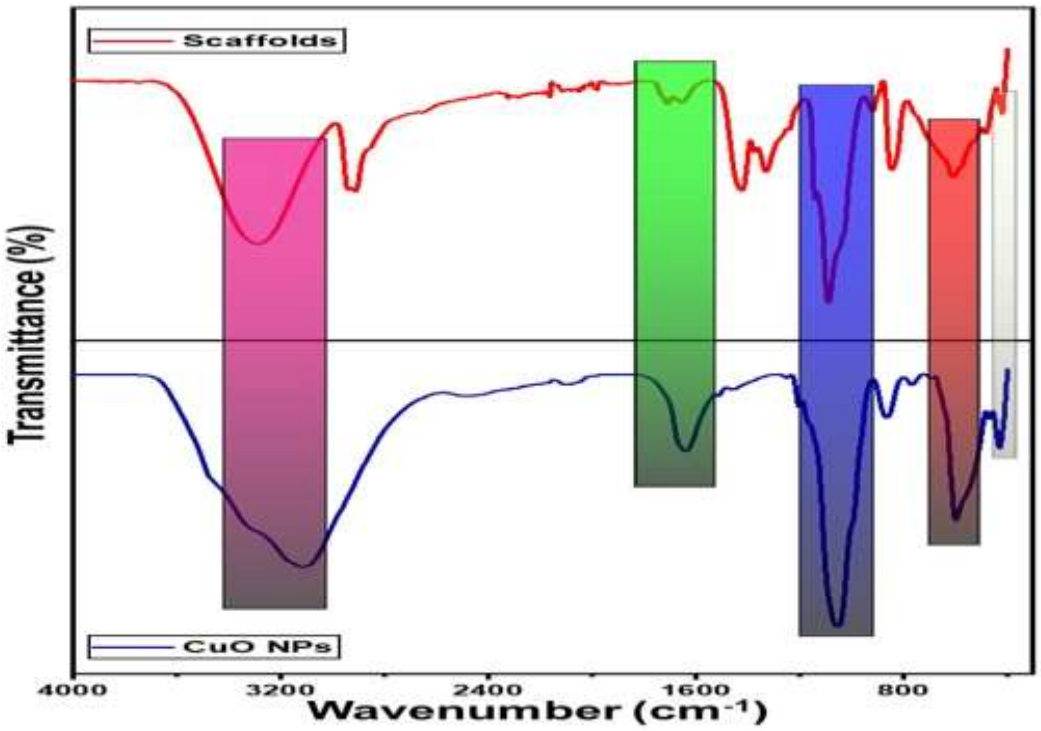

Fig. 2. FTIR spectra of CuO NPs and their incorporation into nanoscaffolds.

3.3. XRD analysis

XRD analysis (Fig. 3) was conducted to examine the crystalline architecture of CuO NPs and their integration into the starch/PVA composite. The CuO NPs exhibited sharp diffraction peaks at 2θ angles of 14.03°, 15.60°, 16.25°, and 24.17°, which align with the monoclinic crystalline phase of CuO, in accordance with JCPDS card No. 48-1548. The most intense diffraction was noted at 24.17° (d-spacing: 3.68 Å), indicating high crystallinity. The starch/PVA scaffold showed broad peaks around 21.35° and 29.30°, which are indicative of the semicrystalline nature of these biopolymers. Weaker signals at 35.78° and 48.52° validated the successful dispersion of CuO NPs within the matrix. The peak broadening observed (FWHM between 0.1° and 0.6°) suggested reduced crystallinity due to nanoparticle-polymer interactions. These diffraction findings confirm that CuO NPs were effectively integrated without compromising the phase stability, an essential trait for biomedical materials.

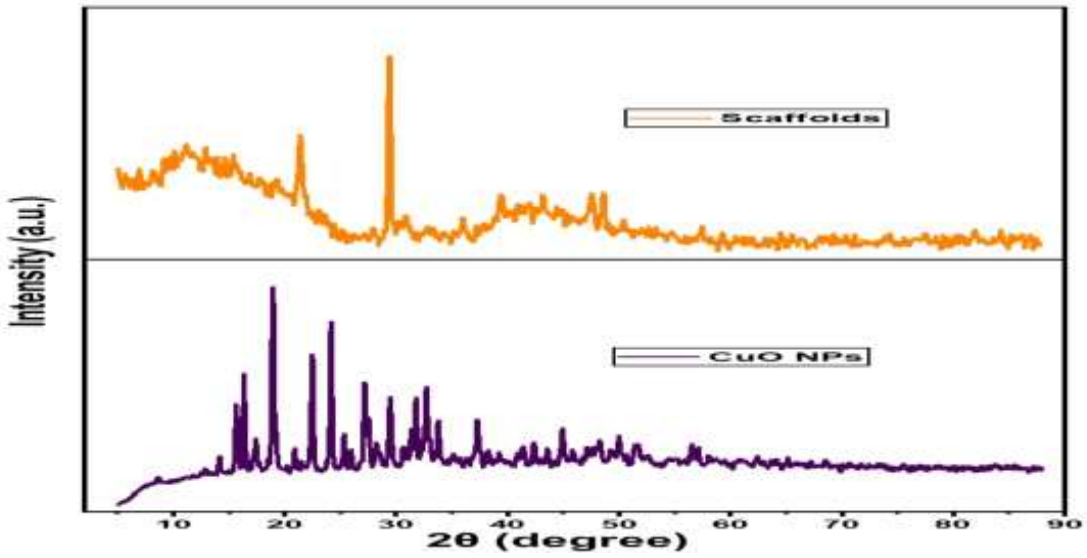

Fig. 3. XRD patterns of synthesized CuO NPs and CuO-loaded scaffolds.

3.4. SEM analysis

SEM (Fig. 4) was utilized to study the topographical features and nanoparticle dispersion in electrospun starch/PVA nanofibers. The CuO NPs appeared largely spherical with minor clumping, likely due to intrinsic surface energy. The nanofibers formed a continuous, well-oriented structure at the nanoscale. Distinct bright particles embedded in the fibers indicated the presence of CuO NPs, verifying uniform integration throughout the

scaffold. The fiber surfaces remained relatively smooth, with minor surface irregularities, suggesting a good interfacial interaction between the CuO NPs and the polymer. Minimal bead formation and steady fiber diameters further reflect optimized electrospinning conditions. These observations validate that the CuO NPs were evenly distributed across the scaffold without disrupting the nanofibrous morphology, supporting their potential in biomedical applications.

3.5. TGA

Thermal stability of the nanofiber scaffolds infused with CuO NPs was evaluated using TGA under a nitrogen environment (Fig. 5). An initial weight reduction of 7.30% occurred below 101.7°C, attributed to moisture loss. The primary thermal decomposition took place from 234.95°C to 377.09°C, with the maximum degradation observed at 324.79°C, corresponding to the breakdown of the starch/PVA matrix and contributing to a 37.37% mass loss. Beyond 400°C, weight reduction proceeded gradually, likely due to carbonaceous material formation and the thermal endurance of CuO NPs. The remaining mass stayed stable up to 548.4°C, indicating improved thermal resilience conferred by the incorporated nanoparticles. These findings suggest that embedding CuO NPs enhances the scaffold's heat stability, a desirable property for high-temperature biomedical and industrial settings.

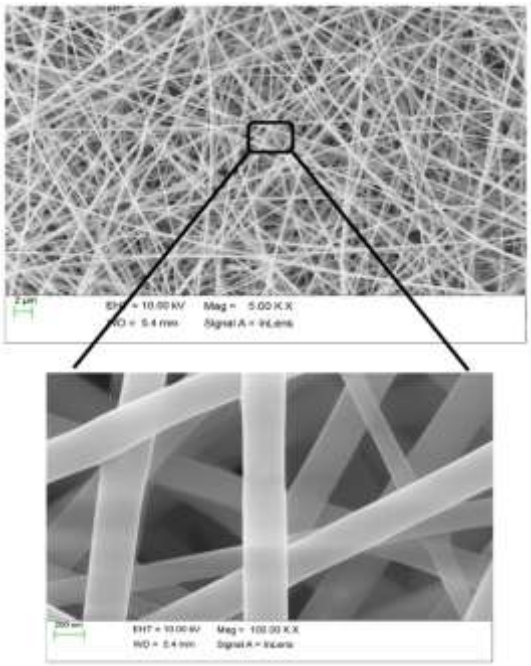

Fig. 4. SEM analysis of fabricated starch/PVA/CuO-NPs nanoscaffolds.

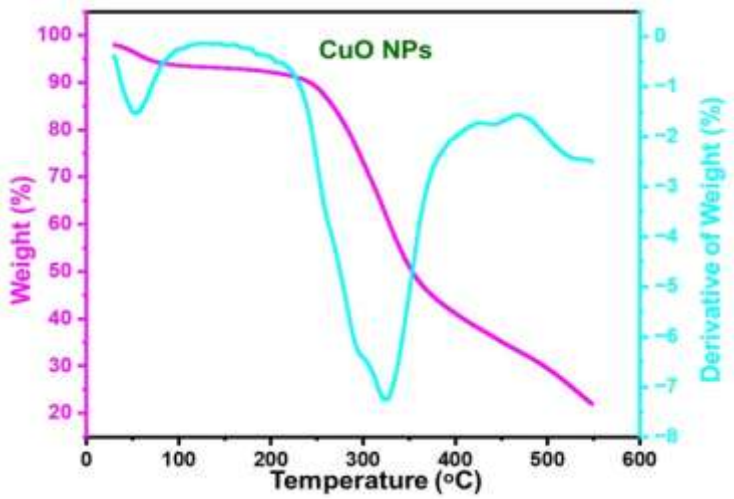

Fig. 5. Thermal degradation behavior of CuO-incorporated nanoscaffolds.

3.6. Zeta potential and particle size analysis

DLS and zeta potential evaluations were conducted to determine the hydrodynamic size and surface charge stability of the synthesized CuO NPs. The average particle size was found to be 92.8 nm (Fig. 6), with a polydispersity index (PDI) of 0.688, indicating moderate variation in particle sizes. Zeta potential measurements (Fig. 7) revealed a mean surface charge of −20.08 mV, with individual peaks at −37.52 mV and −16.29 mV. The

notably negative surface charge implies sufficient electrostatic repulsion to avoid aggregation, ensuring good colloidal stability. The system's conductivity was recorded at 0.0343 mS/cm, and the quality factor measured at 6.538, reflecting dependable data accuracy. These metrics collectively demonstrate that the CuO NPs exhibit adequate dispersion stability, making them appropriate for biomedical uses that require consistent nanoparticle behavior in aqueous environments.

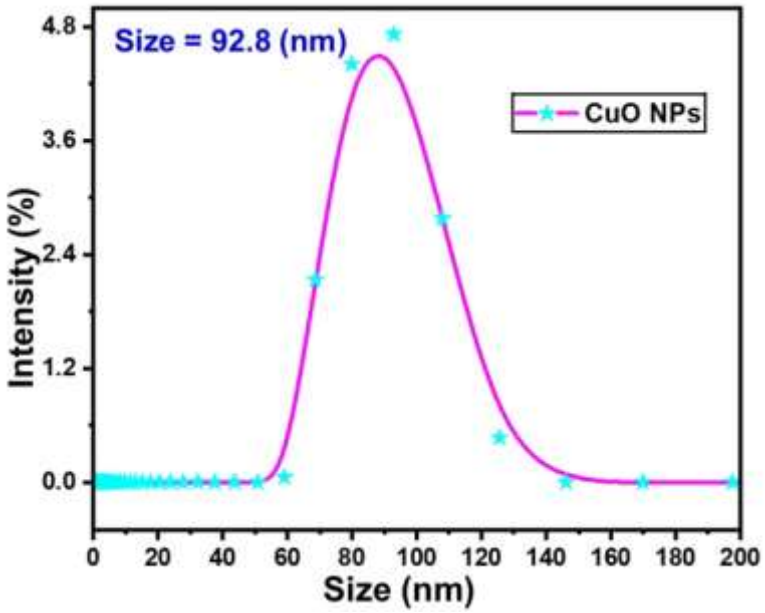

Fig.6. DLS particles size analysis of CuO NPs

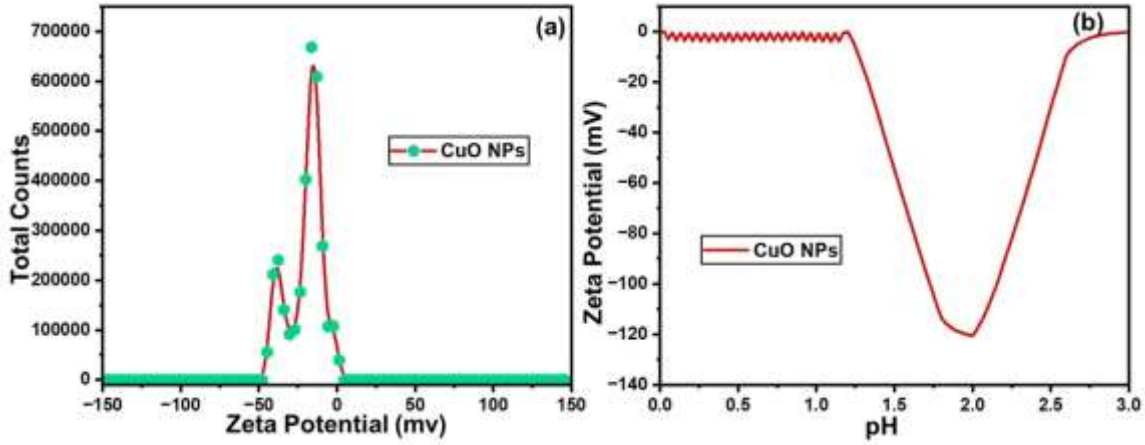

Fig.7. Zeta-potential analysis of CuO NPs

3.7. Wound healing (scratch) assay

The wound healing (scratch) assay (Fig. 8) demonstrated significant differences in the migratory behavior of HaCaT keratinocyte cells after 48 hours of treatment with algal extract, CuO NPs, and starch/PVA/CuO-NPs nanoscaffolds. At the lowest concentration (6.25 µg/mL), the algal extract exhibited a wound closure rate of 35.07%, while CuO NPs and nanoscaffolds showed higher closure rates of 43.07% and 50.07%, respectively. As the concentration increased to 12.5 µg/mL, the algal extract improved to 42.07%, whereas CuO NPs and nanoscaffolds further enhanced wound closure to 49.07% and 65.07%, respectively.

At 25 µg/mL, the algal extract achieved 53.07% wound closure, while CuO NPs and nanoscaffolds displayed even greater efficacy, reaching 65.07% and 76.07%, respectively. The trend continued at 50 µg/mL, where the algal extract resulted in 63.07% closure, compared to 67.07% for CuO NPs and 82.07% for nanoscaffolds. The highest concentration (100 µg/mL) revealed the most pronounced effects: the algal extract reached 72.07% wound closure, CuO NPs achieved 86.07%, and nanoscaffolds exhibited the highest closure rate of 98.07%.

The results indicate a concentration-dependent enhancement in wound healing across all treatments. Notably, the starch/PVA/CuO-NPs nanoscaffolds consistently outperformed both the algal extract and CuO NPs alone at every concentration, suggesting a synergistic effect of the composite material in promoting cell migration. CuO NPs also demonstrated superior activity compared to the algal extract, highlighting the potential of nanoparticle-based treatments in wound repair. The control group (untreated cells) showed minimal migration, confirming that the observed effects were due to the treatments. These findings underscore the therapeutic potential of nanoscaffolds

and CuO NPs in accelerating wound closure, with nanoscaffolds emerging as the most effective formulation for enhancing keratinocyte migration in vitro.

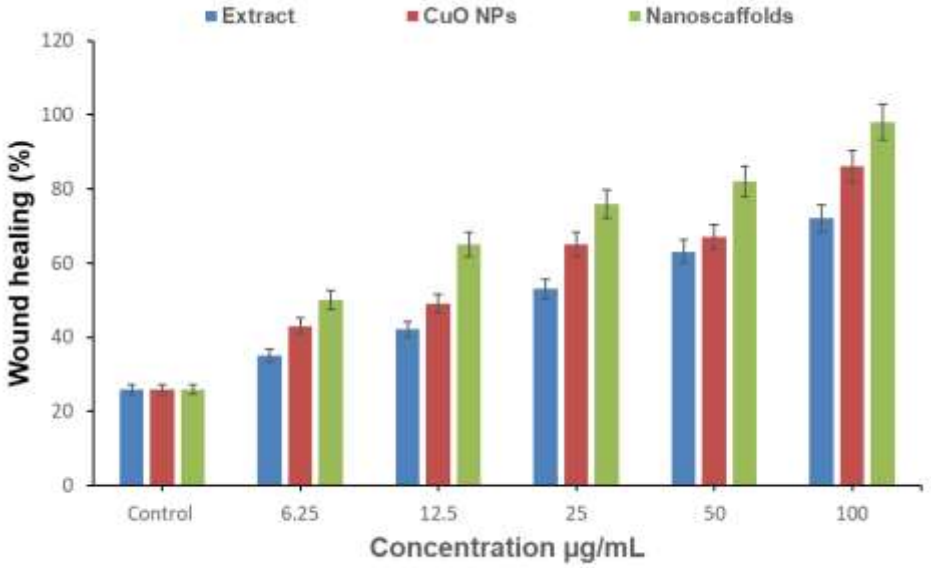

Fig.8. Wound healing activity analysis of algal extract, CuNPs and starch/PVA/CuONPs nanoscaffolds

4. DISCUSSION

The findings of this study clearly demonstrate the successful biosynthesis and functional incorporation of CuO NPs derived from Dictyota algal extract into starch/PVA-based electrospun nanofibrous scaffolds. Each characterization technique provided compelling evidence of nanoparticle formation, stability, and effective embedding within a biopolymer matrix, underscoring the composite's potential for wound healing applications.

The UV–Visible spectroscopic analysis was pivotal in confirming the formation of CuO NPs. The distinct absorption peak observed between 270–300 nm aligns well with previously reported surface plasmon resonance (SPR) features characteristic of CuO NPs. Moreover, the significant absorption band at 337 nm in the algal extract is indicative of phenolic and flavonoid compounds, which likely played dual roles as reducing and capping agents during nanoparticle synthesis. This bioinspired approach underscores the eco-friendly nature of the nanoparticle production process and affirms the active involvement of Dictyota phytoconstituents in nanoparticle formation [42-49].

FTIR spectroscopy provided further insights into the functional groups associated with both CuO NPs and the composite scaffolds. In the CuO spectrum, the appearance of bands corresponding to Cu–O stretching confirms the nanoparticle's metal oxide structure. Meanwhile, the retention of characteristic starch and PVA peaks in the nanoscaffold spectrum implies that the overall chemical integrity of the polymeric matrix was not compromised upon nanoparticle integration. The subtle presence of CuO-related peaks in the scaffold spectrum suggests that the nanoparticles were successfully embedded within the biopolymer network, maintaining essential functional moieties [50-58].

Crystallographic studies via XRD corroborated the phase purity and crystallinity of the synthesized nanoparticles. The diffraction peaks of the CuO NPs matched the monoclinic phase (JCPDS No. 48-1548), with sharp, intense signals indicating high crystallinity. Interestingly, the polymeric scaffolds displayed broad peaks corresponding to the semi-crystalline nature of starch and PVA. The emergence of minor CuO-specific peaks within the scaffold's diffractogram affirms that the nanoparticles were uniformly distributed throughout the matrix without altering its phase behavior. Peak broadening in the composite, as indicated by full width at half maximum (FWHM) values, likely reflects reduced crystallinity due to interactions between polymer chains and embedded nanoparticles [59-65].

The morphological assessment through SEM revealed well-formed, continuous nanofibers with embedded nanoparticles clearly visible as discrete bright spots. The spherical morphology of CuO NPs, along with minimal aggregation, attests to successful capping by phytochemicals and homogenous dispersion within the fibers. Importantly, the nanofibers retained structural integrity with negligible bead formation, highlighting optimal electrospinning conditions and the compatibility of CuO NPs with the polymer solution. The uniform surface morphology is particularly crucial for biomedical scaffolds, as it influences cellular adhesion and proliferation [66-69].

Thermal analysis via TGA provided critical information about the composite's stability under elevated temperatures. The enhanced thermal stability observed in CuO-containing nanoscaffolds—evidenced by delayed onset of degradation and greater residual mass—can be attributed to the intrinsic high-temperature endurance of metal oxide nanoparticles. The initial weight loss due to moisture evaporation and subsequent decomposition

phases of starch and PVA were clearly demarcated, confirming that nanoparticle incorporation enhanced the material's resistance to thermal decomposition. Such thermal resilience is desirable for storage and sterilization of biomedical materials [70].

Furthermore, DLS and zeta potential analyses verified the colloidal stability and size uniformity of the biosynthesized CuO NPs. The average particle size (~92.8 nm) falls within the optimal nanoscale range for biomedical applications. The moderate polydispersity index (PDI = 0.688) implies some degree of size variation, which is acceptable in biogenic syntheses. More importantly, the negative zeta potential (−20.08 mV) suggests adequate surface charge to maintain dispersion stability, thereby preventing aggregation. This feature is particularly important for biomedical formulations where consistent nanoparticle behavior in physiological environments is necessary [71, 72].

The in vitro wound healing assay provided perhaps the most compelling evidence of the composite scaffold's biomedical potential. All treatments—Dictyota extract, CuO NPs, and the nanoscaffolds—exhibited a concentration-dependent increase in keratinocyte migration, with the nanoscaffold formulation consistently outperforming the others. At all concentrations tested, the composite scaffolds showed superior wound closure rates, reaching up to 98.07% at 100 µg/mL. This marked enhancement likely results from the synergistic effect of the biocompatible polymeric matrix providing a structural framework for cell growth, combined with the antimicrobial and pro-healing properties of CuO NPs. The CuO NPs alone outperformed the algal extract, suggesting that the nanoparticle form enhances bioactivity, possibly through increased surface area and improved cellular interaction. The control group's poor performance underscores the efficacy of the treatments [73, 74].

Collectively, these results validate the strategic integration of green-synthesized CuO NPs into starch/PVA scaffolds for wound healing. The combination leverages the biological activity of marine algae, the physicochemical robustness of CuO NPs, and the biocompatibility of natural polymers to yield a multifunctional nanocomposite. This material offers promising prospects for future clinical applications in tissue engineering and regenerative medicine.

5. CONCLUSION

This study successfully demonstrated the fabrication and therapeutic potential of starch/PVA nanoscaffolds embedded with green-synthesized CuO NPs derived from Dictyota sp. extract for enhanced wound healing. Comprehensive characterization via UV-Vis, FTIR, XRD, SEM, and TGA confirmed the successful formation, structural integrity, and thermal stability of the CuO NPs and their uniform integration into the nanofibrous scaffold. The wound healing assay revealed a concentration-dependent response, with starch/PVA/CuO-NP nanoscaffolds exhibiting superior efficacy (98.07% closure at 100 µg/mL) compared to standalone CuO NPs (86.07%) and algal extract (72.07%). The enhanced performance of the nanoscaffold can be attributed to the synergistic effects of the bioactive CuO NPs and the biocompatible polymeric matrix, which collectively promote keratinocyte migration and wound closure. These findings highlight the potential of eco-friendly, algae-mediated CuO NPs and their incorporation into biodegradable nanoscaffolds as a promising strategy for advanced wound care. Future studies should focus on in vivo validation and long-term biocompatibility to facilitate clinical translation.

Ethical Declaration: Not Applicable

Data Availability Statement: The full dataset of physiochemical characterization associated with this work is published in Mendeley Data [Dataset] Multidisciplinary evaluation of biofabricated starch nanoscaffolds incorporating phyto-synthesized CuO nanoparticles from *Dictyota* extract (DOI: 10.17632/xtwhbc25hj.1).
Disclosure: The material characterization data and figures (e.g., UV, SEM, FTIR, XRD, TGA, Zeta Potential and particle sizer) presented here were generated from a common dataset and are being reused across multiple related studies on nanomaterials. All biological analyses and conclusions are original to each manuscript.

Conflicts of Interest: The authors declare no conflicts of interest.

REFERENCES

[1] Raju M, Chandrasekaran MK, Loganathan L, Ahalliya RM, Mironescu M, Mironescu ID, Palanisamy CP, Kanniappan GV. Lipid remodeling and ferroptosis in phosphatidylcholine-mediated tumor–stroma crosstalk. Frontiers in Molecular Biosciences. 2026; 13: 1742305.

[2] Kunamalla R, Panagal M, Palanisamy CP. Biogenic synthesis and fabrication of starch/PVA/CuO electrospun nanoscaffolds from Sargassum ilicifolium (brown marine macroalgae) extract for anticancer activity on HT-29 and MCF-7 cancer cells. Biocatalysis and Agricultural Biotechnology. 2026; 72: 103923.

[3] Pei J, Govindaraj H, Sivaramakrishnan R, Kanniappan GV, Pandurangan V, Dhayalan VK, Mironescu M, Mironescu ID, Jayaraman S, Palanisamy PC. Sustainable fabrication of biopolymer-based (starch/PVA) nanoscaffolds loaded with green-synthesized CuO nanoparticles from Sargassum wightii (marine macroalgae): Cytocompatibility and antioxidant activity. Biomaterials Advances. 2026; 182: 214660.

[4] Pei J, Perumal NC, Meng P, Long Q, Palanisamy CP. Extracellular vesicle-based biosensors for Alzheimer's disease: A new frontier in precision diagnostics. Ageing Research Reviews. 2026; 113: 102904.

[5] Shree P, Sivaramakrishnan R, Kanniappan GV, Pandurangan V, Jayaraman S, Dhayalan VK, Mironescu M, Mironescu ID, Palanisamy CP. Antioxidant and biocompatible CuO-starch/PVA nanoscaffolds via ultrasonic green synthesis using Turbinaria conoides (brown marine macroalgae). Medicine in Drug Discovery. 2025; 28: 100238.
[6] Gong J, Lin J, Guan T, Pei J, Palanisamy CP, El-AtyFrom AMA. selenium tolerance to nanoplastic antagonism: Comprehensive characterization of L. casei SNUT1 and its extracellular vesicle–nanoselenium complex. Food Bioscience. 2025; 74: 107749.
[7] Poochi SP, Sundarraj R, Raju MV, Chandrasekaran MK, Ahalliya RM, Palanisamy CP, Kanniappan GV, Kondapavuluri BK, Thiruvengadam M. Harnessing Nature: Computational and Experimental Insights Into *Ipomoea obscura* Metabolites for Bladder Cancer Therapy. Chemistry and Biodiversity. 2025; 0: e00909.
[8] Dugganaboyana GK, Kannankumar MKG, Shivaramakrishna S, Raju MV, Chandrasekaran MK, Ahalliya RM, Panneerselvam N, Palanisamy CP, Kanniappan GV. Phytochemical insights, antioxidant activity and therapeutic potential of Cassia senna against prostate cancer in Wistar albino rats. Discover Applied Sciences. 2025; 7:1206.
[9] Natarajan SR, Krishnamoorthy R, Alshuniaber MA, Gatasheh MK, Rajagopal P, Veeraraghavan VP, Palanisamy CP, Jayaraman S. KDM1A Facilitates Oncogenic Potential in Colorectal Cancer Progression Through the Activation of AXIN/GSK3β/β-Catenin Signaling Pathways: Evidence From Integrated Transcriptomics and In Vitro Studies. The Journal of Gene Medicine. 2025; 27(11): e70053.
[10] Guan T, Gong J, Lin J, Palanisamy CP, Jinjin Pei J, El-Aty AMA. Machine learning-driven multimodal optimization of selenium biotransformation and flavor profiling in fermented apple–Yacon functional beverages. Innovative Food Science & Emerging Technologies. 2025; 105: 104198.
[11] Natarajan SR, Krishnamoorthy R, Alshuniaber MA, Alsulami TS, Gatasheh MK, Rajagopal P, Palanisamy CP, Govindan R, Veeraraghavan VP, Jayaraman S. ABCE1 facilitates tumour progression via aerobic glycolysis and inhibits cell death in human colorectal cancer cells through the p53 signalling pathway. Scientific Reports. 2025; 15: 24674.
[12] Huang Y, Guo H, Liu Y, Jin W, Palanisamy CP, Pei J, Oz F, El-Aty AMA. Effects of Natural Polysaccharides on the Gut Microbiota Related to Human Metabolic Health. Molecular Nutrition & Food Research. 2025; 69:e202400792.
[13] Poornima K, Meenakshi K.C, Manikandan V.R, Shankari G, Prabhu D, Rathi M.A, Palanisamy CP, Balaji R, Gopalakrishnan V.K. Exploring the anticancer potential of Jerantinine A from *Tabernaemontana coronaria* against prostate, breast, and ovarian cancers: A computational approach. *Journal of Complementary and Integrative Medicine*, 2025 22(2): 363–372.
[14] Palanisamy CP, Poompradub S, Sansanaphongpricha K, Jayaraman S, Subramani K. Faridah Sonsudin gGreen synthesis of Nigella sativa-mediated silver nanoparticles for enhanced antibacterial activity and wound healing: Mechanistic insights and biomedical applications. Environmental Nanotechnology, Monitoring & Management. 2025; 24: 101085.
[15] Surendran N, Raju MV, Chandrasekaran MK, Ahalliya RM, Palanisamy CP, Chandrasekaran G, Kanniappan GV. Physicochemical characterization of starch from Maranta arundinacea L.(arrowroot) rhizomes and its inhibition of COX-2: In vivo validation. Bioactive Carbohydrates and Dietary Fibre. 2025; 33: 100465.
[16] Kannappan P, Chandrasekaran MK, Raju MV, Gopalakrishnan S, Dhamodharan P, Ahalliya RM, Palanisamy CP, Raju B, Kanniappan GV. Exploring the anticancer potential of Jerantinine A from Tabernaemontana coronaria against prostate, breast, and ovarian cancers: a computational approach. Journal of Complementary and Integrative Medicine. 2025; 22(02): 363-372.
[17] Pei J, Kumarasamy RV, Jayaraman S, Kanniappan GV, Long Q, Palanisamy CP. Quercetin-functionalized nanomaterials: Innovative therapeutic avenues for Alzheimer's disease management. Ageing Research Reviews. 2025; 104: 102665.
[18] Jayaraman S, Prasad M, Natarajan SR, Krishnamoorthy R, Alshuniaber MA, Gatasheh MK, Veeraraghavan VP, Rajagopal P, Palanisamy CP. Molecular mechanisms underlying the effects of beta-sitosterol on TGF-β1/Nrf2/SIRT1/p53-mediated signaling in the kidney of a high-fat diet and sucrose-induced type-2 diabetic rat. Chemico-Biological Interactions. 2025; 411: 111443.
[19] Huang Y, Guo H, Liu Y, Jin W, Palanisamy CP, Pei J, Oz F, El-Aty AMA. Effects of Natural Polysaccharides on the Gut Microbiota Related to Human Metabolic Health. Molecular Nutrition & Food Research. 2025; e202400792.
[20] Prabhakaran P, Palanisamy CP, Shanmugam A, Damodharan P, Swaminathan H, Devaraj D, Ahalliya RM, Kanniappan GV. Isolation, structural characterization, and molecular docking studies on the bioactive compound from n-Hexane extract of Emilia sonchifolia (L.) DC against the pancreatic cancer target Aurora 2 Kinase. Journal of Complementary and Integrative Medicine. 2024; 22(1): 0290.
[21] Jiang H, Kumarasamy RV, Pei J, Raju K, Kanniappan GV, Palanisamy CP. Integrating engineered nanomaterials with extracellular vesicles: Advancing targeted drug delivery and biomedical applications. Frontiers in Nanotechnology. 2024; 6: 1513683.
[22] Guo H, Liu Y, Wan T, Song D, Palanisamy CP, Geng J, Pei J, Özmen S, El-Aty AMA. Toward personalized cancer management: Role of precision nutrition–diet interventions. Journal of Functional Foods. 2024; 123: 106584.

[23] Natarajan SR, Krishnamoorthy R, Alshuniaber MA, Al-Anazi KM, Farah MA, Rajagopal P, Palanisamy CP, Veeraraghavan VP, Jayaraman S. Identification of FOXM1 as a novel protein biomarker and therapeutic target for colorectal cancer progression: Evidence from immune infiltration and bioinformatic analyses. International Journal of Biological Macromolecules. 282 (Part 4): 137201.
[24] Rajendran MS, Jayaraman S, Khan JM, Jasmine S, Prabhakaran RK, Raju MV, Chandrasekaran MK, Ahalliya RM, Kannappan P, Palanisamy CP, Kanniappan GV. Investigating the colon toxicity and carcinogenic role of monosodium glutamate compared with Dimethylhydrazine in male Wistar rats: Exploring the link to childhood colon cancer risk. Journal of King Saud University - Science. 2024; 36(11): 103507.
[25] Kumarasamy RV, Natarajan P, Umapathy VR, Roy JR, Rab SO, Saeed M, Panagal M, Mironescu M, Srinivasan GP, Palanisamy CP. Clinical Applications and Therapeutic Potentials of Advanced Nanoparticles: A Comprehensive Review on Completed Human Clinical Trials. Frontiers in Nanotechnology. 2024; 6:1479993.
[26] Jin W, Pei JJ, Roy JR, Jayaraman S, Ahalliya RM, Kanniappan GV, Mironescu M, Palanisamy CP. Comprehensive review on single-cell RNA sequencing: A new frontier in Alzheimer's disease research. Ageing Research Reviews. 2024; 274: 102454.
[27] Pei J, Palanisamy CP, Jayaraman S, Natarajan PM, Umapathy VR, Roy JR, Panagal M, Jayaraman S. Curcumin-loaded polymeric nanomaterials as a novel therapeutic strategy for Alzheimer's disease: A comprehensive review. Ageing Research Reviews. 2024; 99: 102393.
[28] Pei J, Palanisamy CP, Jayaraman S, Natarajan PM, Umapathy VR, Roy JR, Thalamati D, Ahalliya RM, Kanniappan GV, Mironescu M. A comprehensive review on starch-based Sustainable Edible Films Loaded with Bioactive Components for Food Packaging. International Journal of Biological macromolecules. 2024; 274 (Part-1): 133332.
[29] Palanisamy CP, poompradub S, Sansanaphongpricha K, Subramani K, Sonsudin F. Increased expression levels of PDGF and VEGF magnify the wound healing potential facilitated by biogenic synthesis of silver nanoparticles. Nano-Structures & Nano-Objects. 2024; 39: 101236.
[30] Pei J, Palanisamy CP, Jayaraman S, Natarajan PM, Umapathy VR, Roy JR, Thalamati D, Ahalliya RM, Kanniappan GV, Mironescu M. Proteomics Profiling of Extracellular Vesicle for Identification of Potential Biomarkers in Alzheimer's Disease: A Comprehensive Review. Ageing Research Reviews. 2024; 99: 102359.
[31] Xi J, Wang T, Xian P, Liu X, Du M, Yang H, Palanisamy CP, Lin W, Long Q. Proteomic insights uncover enhanced neurotherapeutic potential in conditioned mesenchymal stem cell-derived extracellular vesicles. Extracellular Vesicle. 2024; 3: 100037.
[32] Pei J, Natarajan PM, Umapathy VR, Swamikannu B, Sivaraman NM, Krishnasamy L, Palanisamy CP. Advancements in the synthesis and functionalization of zinc oxide-based nanomaterials for enhanced oral cancer therapy. Molecules. 2024; 29(11): 2706.
[33] Gatasheh MK, Natarajan SR, Krishnamoorthy R, Alsulami TS, Rajagopal P, Palanisamy CP, Veeraraghavan VP, Jayaraman S. Molecular analysis to identify novel potential biomarkers as drug targets in colorectal cancer therapy: an integrated bioinformatics analysis. Molecular and Cellular Oncology. 2024; 11(1): 2326699.
[34] Pei J, Yan Y, Jayaraman S, Rajagopal P, Natarajan PM, Umapathy VR, Gopathy S, Roy JR, Sadagopan CS, Thalamati D, Palanisamy CP, Mironescu M. A review on advancements in the application of starch-based nanomaterials in biomedicine: Precision drug delivery and cancer therapy. International Journal of Biological Macromolecules. 2024; 130746.
[35] Pei JJ, Yan Y, Palanisamy CP, Jayaraman S, Natarajan PM, Umapathy VR, Gopathy S, Roy JR, Sadagopan JC, Thalamati D, Mironescu M. Materials-based drug delivery approaches: Recent advances and future perspectives. Green Processing and Synthesis. 2024; 13: 20230094.
[36] Pei JJ, Deng W, Liu Y, Guo Y, Chen J, Abdu H, Khan MR, Palanisamy CP, El-Aty AM. A Comprehensive Review of Cornus officinalis: Health Benefits, Phytochemistry, and Pharmacological Effects for Functional Drug and Food Development. Frontiers in Nutrition. 2023; 10: 1309963.
[37] Alugoju P, Palanisamy CP, Anthikapalli NVA, Jayaraman S, Prasanskulab A, Chuchawankul S, Dyavaiah M, Tencomnao T. Exploring the anti-aging potential of natural products and plant extracts in budding yeast Saccharomyces cerevisiae: A review. F1000Research. 2023; 12: 1265.
[38] Lavanya M, Krishnamoorthy R, Alshuniaber MA, Manoharadas S, Palanisamy CP, Veeraraghavan VP, Jayaraman S, Rajagopal P, Padmini R. Formulation, characterization and evaluation of gelatin-syringic acid/zinc oxide nanocomposite for its effective anticancer, antioxidant and anti-inflammatory activities. Journal of King Saud University-Science. 2023; 35: 102909.
[39] Palanisamy CP, Poompradub S, Sansanaphongpricha K, Jayaraman S, Subramani K, Sonsudin F. Biosynthesis of silver nanoparticles (AgNPs) using ethanolic extract of Nigella sativa (L.) seeds promotes wound healing via PDGF and VEGF signalling pathways activation. Biocatalysis and Agricultural Biotechnology. 2023; 54: 102970.
[40] Natarajan PM, Umapathy VR, Murali A, Swamikannu B. (2022). Computational Simulations of Identified marine-derived Natural Bioactive Compounds As Potential Inhibitors of Oral Cancer. Future Science OA. 2022; 8(3).
[41] Natarajan PM, Umapathy VR. Role of transcriptomics in the study of oral cancer. Frontiers in Oral Health. 2025; 6:1524364.

[42] Vidhyarekha U, Natarajan PM, Bhuminathan S, Sabarinathan J, Suba R, Vijayalakshmi P. Role of artificial intelligence in Oral Cancer. Advances in Public Health. 2024. 2024: 3664408.
[43] Ganesan A, Kumar NG, Natarajan PM, Gauthaman J. Automated classification of elongated styloid processes using deep learning models-an artificial intelligence diagnostics. Frontiers in Oral Health. 2025; 5: 1424840.
[44] Umapathy VR, Natarajan PM, Swamikannu B. Regenerative Strategies in Dentistry: Harnessing Stem Cells, Biomaterials and Bioactive Materials for Tissue Repair. Biomolecules. 2025; 15: 546.
[45] Natarajan PM. Dental Bioinformnatics-Current Scope and Future perspectives. Research Journal of Pharmacy and Technology. 2022;15(5):2351-6.
[46] Ganesan A, Kumar NG, Natarajan PM. Solanum trilobatum leaf extract-derived silver nanoparticles downregulate the PI3K/AKT/mTOR signaling pathway and attenuate oral squamous cell carcinoma cell proliferation. Journal of Herbmed Pharmacology. 2024; 13(2): 300-307.
[47] Perumal MKK, Renuka RR, Subbiah SK, Natarajan PM. Artificial intelligence-driven clinical decision support systems for early detection and precision therapy in oral cancer: a mini review. Frontiers in Oral Health. 2025; 6: 1592428.
[48] Ramesh E, Ganesan A, Lakshmi KC, Natarajan PM. Artificial intelligence-based diagnosis of oral leukoplakia using deep convolutional neural networks Xception and MobileNet-v2. Frontiers in Oral Health. 2025; 6: 1414524.
[49] Ganesan A, Kumar NG, Natarajan PM. Anticancer activity of silver nanoparticles synthesized from aqueous leaf extract of Solanum trilobatum (Purple fruit pea eggplant) on human oral cancer cells. Journal of Herbmed Pharmacololgy. 2024; 13(2): 260-268.
[50] Natarajan PM, Swamikannu B, Sivaraman NM, Stylin AGSQ. Prevention of Oral Cancer: A Comprehensive Guide. Journal of Pharmacy and Bioallied Sciences. 2024; 16(5): S4239-S4241.
[51] Umapathy V, Dhanavel A, Kesavan R, Natarajan PM, Bhuminathan S, Vijayalakshmi P. Anticancer Potential of the Principal Constituent of Piper nigrum, Piperine: A Comprehensive Review. Cureus. 2024; 16(2): e54425.
[52] Umapathy VR, Swamikannu B, Natarajan PM, Devi R, Nandini MS, Vimalarani, Vijayalakshmi P. In Silico Molecular Docking of Ocimum sanctum Phytochemicals: Targeting Key Biomarkers in Oral Cancer. Journal of Pharmacy and Bioallied Sciences. 2024; 16(5): S4792-S4799.
[53] Natarajan PM, Bhuminathan S, Rajan R, Bindu K, Loganathan K, Veerakumar R. The Crucial Role of Smoking Cessation in Preventing Oral Cancer. Journal of Pharmacy and Bioallied Sciences. 2024; 16(5): S4245-S4247.
[54] Swamikannu B, Umapathy VR, Natarajan PM, Nandini MS, Stylin AGSQ, Vimalarani V, Rajinikanth S. Unlocking the Therapeutic Benefits of Artemisia Annua: A Comprehensive Overview of its Medicinal Properties. Journal of Pharmacy and Bioallied Sciences. 2024; 16(5): S4248-S4253.
[55] Natarajan PM. Computational Studies on Recent Congeners of Fluoroquinolones and Nitroimidazoles for Their Use in Periodontal Therapy. Journal of Pharmacy and Bioallied Sciences. 2024; 16(5): S4731-S4740.
[56] Yadalam PK, Arumuganainar D, Natarajan PM, Ardila CM. Artificial intelligence-powered prediction of AIM-2 inflammasome sequences using transformers and graph attention networks in periodontal inflammation. Scientific Reports. 2025; 15: 8733.
[57] Yadalam PK, Chatterjee S, Natarajan PM, Ardila CM. Comparison of light gradient boosting and logistic r egression for interactomic hub genes in Porphyromonas gingivalis and Fusobacterium nucleatum-induced perio dontitis with Alzheimer's disease. Frontiers in Oral Health. 2025; 6:1463458.
[58] Natarajan PM, Bhuminathan S, Leela B, Bindu K, Loganathan K, Ramachandran V. Smoking and its Role in Oral Cancer. Journal of Pharmacy and Bioallied Sciences 16(5): S4242-S4244.
[59] Yadalam PK, Natarajan PM, Ardila CM. Variational graph autoencoder for reconstructed transcriptomic data associated with NLRP3 mediated pyroptosis in periodontitis. Scientific Reports. 2025; 15: 1962.
[60] Daniel Raja FS, Abraham L, Rangasamy K, Saikia K, Rathankumar AK, Mironescu M, Mironescu I, Palanisamy CP, Kanniappan GV. Next-Generation Microbiome Therapeutics: Psychobiotics and Fecal Microbiota Transplants (FMT) for Mental Health Treatment. Frontiers in Cellular and Infection Microbiology. 2026; 16: 1719357.
[61] Dharmaprakash S, Gunasekaran VP, Sivaramakrishnan R, Kanniappan GV, Jayaraman S, Mironescu M, Rajabathar JR, Mironescu ID, Palanisamy CP. Marine macroalgae-mediated ultrasonic-assisted green synthesis of CuO nanoparticles embedded in starch/PVA electrospun nanoscaffolds for in vitro α-amylase and α-glucosidase inhibitory activity. Scientific Reports. 2026.
[62] Surendran N, Chandrasekaran G, Raju MV, Chandrasekaran MK, Ahalliya RM, Palanisamy CP, Kanniappan GV, Arcot R, Alharbi NS, Thiruvengadam M. Anti-inflammatory potential of ethanolic extract of Maranta arundinacea L.: Insights from COX-2 modulation and oxidative stress analysis. South African Journal of Botany. 2026; 195: 142-151.
[63] Pei J, Senthilkumar MV, Hessini K, Subramaniyam S, Sivaramakrishnan R, Kanniappan GV, Jayaraman S, Palanisamy CP. Green fabrication of starch/PVA/CuO nanoscaffolds using marine macroalgae extract for enhanced anti-inflammatory activity. Sustainable Chemistry and Pharmacy. 2026; 51: 102397.
[64] Balasubramanian V, Loganathan L, Muthuswamy K, Viswanathan TM, Raju MV, Chandrasekaran MK, Ahalliya RM, Poorasamy J, Palanisamy CP, Dominic S, Kanniappan GV. Anticancer therapeutic efficacy of

PEGylated β-galactosidase from Aspergillus terreus in DMBA-induced breast cancer: Toxicological, molecular and histopathological evaluation in Wistar rats. International Journal of Biological Macromolecules. 2026; 360: 151856.
[65] Jayaraman S, Eswaran A, Rajagopal P, Palanisamy CP, Veerakumar P, Veeraraghavan VP, Sirasanagandla SR. Neuroendocrine-associated epigenetic factors in cellular senescence: mechanisms and therapeutic implications. Biogerontology. 2026; 27(2): 64.
[66] Ponnusamy B, Rajagopal P, Palanisamy CP, Veeraraghavan VP, Jayaraman S. Mechanistic Exploration of the anticancer activity of Justicia adhatoda Plant Leaf Ethanolic Extract against Colon Cancer Cells: An in silico and in vitro Approach. Asian Pacific Journal of Cancer Prevention. 2026; 27(3): 1069-1080.
[67] Pei J, Saran VS, Sivaramakrishnan R, Kanniappan GV, Pandurangan V, Jayaraman S, Dhayalan VK, Mironescu M, Mironescu ID, Palanisamy CP. Ultrasonic-assisted, Sargassum ilicifolium (brown marine macroalgae)-mediated biogenic synthesis of CuO nanoparticles incorporated in starch/PVA electrospun nanoscaffolds: In vitro safety and antioxidant efficacy assessment. Bioorganic Chemistry. 2026; 173: 109679.
[68] Raj MAPA, Subramaniyam S, Kanniappan GV, Jayaraman S, Palanisamy CP. Sustainable fabrication of starch/PVA/CuO electrospun nanoscaffolds from Turbinaria ornata (marine macroalgae) extract: Physicochemical characterization and antidiabetic evaluation. Kuwait Journal of Science. 2026; 53(2): 100545.
[69] Pei J, Ganesh NS, Subramaniyam S, Sivaramakrishnan R, Kanniappan GV, Jayaraman S, Palanisamy CP. Sustainable fabrication of starch/PVA/CuO electrospun nanoscaffolds from Padina tetrastromatica (Brown macroalgae) extract: Physicochemical characterization and antidiabetic assessment. Sustainable Chemistry One World. 2026; 9: 100195.
[70] Sakthiraj A, Sivaramakrishnan R, Subramaniyam S, Kanniappan GV, Pandurangan V, Jayaraman S, Dhayalan VK, Mironescu M, Mironescu ID, Palanisamy CP. Starch/PVA electrospun nanoscaffolds loaded with ultrasonic-assisted green-synthesis of CuO nanoparticles from marine macroalgae (Gracilaria corticata) extract: Cytotoxicity and antioxidant analysis. Chemical Physics Impact. 2026; 12: 101018.
[71] Prasad M, Jayaraman S, Natarajan SR, Veeraraghavan VP, Krishnamoorthy R, Gatasheh MK, Palanisamy CP, Elrobh M. Piperine modulates IR/Akt/GLUT4 pathways to mitigate insulin resistance: Evidence from animal and computational studies. International Journal of Biological Macromolecules. 2023; 253: 127242.
[72] Palanisamy CP, Pei JJ, Phaniendra A, Venkata AAN, Jayaraman S, Veeraragahavan VP, Sridevi G, Roy JR, Janaki CS, Thalamati D, Mironescu M, Luo Q, Chai Y, Long Q. New Strategy of Neurodegenerative Disease Treatment with Extracellular Vesicles (EVs) Derived from Mesenchymal Stem Cells (MSCs). *Theranostics*. 2023; 13(12):4138-4165. doi:10.7150/thno.83066.
[73] Palanisamy CP, Phaniendra A, Jayaraman S, Poompradub S. *Nigella sativa* L. seed extracts promotes wound healing progress by activating VEGF and PDGF signalling pathways: *An in vitro* and *in silico* study. *F1000 Research*. 2023; 12: 436.
[74] Pei JJ, Palanisamy CP, Phaniendra A, Venkata AAN, Natarajan PM, Umapathy VR, Swamikannu B, Jayaraman S, Rajagopal P, Poompradub S. A comprehensive review on bio-based materials for chronic diabetic wounds. *Molecules*. 2022; 28(2), 604.